Experimental Heat Transfer, vol. 4, pp. 217–233, 1991

SIMULTANEOUS MEASUREMENTS OF THICKNESS AND TEMPERATURE PROFILE IN A WAVY LIQUID FILM FALLING FREELY ON A HEATING WALL

Tae-hwan Lyu and Issam Mudawar
Boiling and Two-Phase Flow Laboratory, School of Mechanical Engineering, Purdue University, West Lafayette, Indiana 47907

A technique for measuring the thickness of liquid films was developed and successfully tested. The feasibility of this technique was demonstrated in stagnant liquid films as well as in liquid jets. A procedure for in-situ calibration of the thickness probe was developed, allowing the adaptation of the probe to measurements of wavy liquid films. The thickness probe was constructed from a platinum-rhodium wire that was stretched across the film. A constant DC current was supplied through the probe wire, and film thickness was determined from variations in the probe voltage drop resulting from the large differences in the electrical resistances of the wetted and unwetted segments of the wire. Unlike electrical admittance thickness probes, the new probe did not require dissolving an electrolyte in the liquid, making the new probe well suited to studies involving sensible heating of a film of pure dielectric liquid that is in direct contact with a current-carrying wall. Also presented is a composite probe that facilitated simultaneous measurements of temperature profile across a wavy liquid film and film thickness. Experimental results demonstrate a strong influence of waviness on liquid temperature in a film of deionized water falling freely on the outside wall of a vertical, electrically heated tube for film Reynolds numbers smaller than 10,000.

INTRODUCTION

Thin liquid films are encountered in many types of industrial thermal and chemical process equipment, such as thin-film evaporators, plate-type condensers, distillation columns, and gas-absorption devices. Numerous efforts have been undertaken during the last seven decades to model thin-film flows in order to develop reliable predictive tools for the design and performance assessment of this equipment. Still, there are many unanswered questions concerning the physical origins and hydrodynamic features of interfacial waves on a liquid film, and the impact of these waves on the transport processes of mass, momentum, and heat associated with liquid films.

One major reason for the inconclusive understanding of film behavior is the difficulty in performing accurate measurements of a transport variable simultaneously with film thickness. As shown in Fig. 1, determining the heat transfer coefficient associated with sensible heating of a falling film on a vertical wall requires mapping of temperature and velocity across the film, and referencing these variables to film thickness. These

This article is based on work supported by the U.S. Department of Energy, Office of Basic Energy Science, through Grant DE-85ER13398.

NOMENCLATURE

A_c	cross-sectional area of probe wire ($= \pi d^2/4$)	V	voltage
b_a, b_c, b_ℓ	lengths or probe wire segments	x	longitudinal distance from the leading edge of the heater
Bi	Biot number [$= hd/(4k_s)$]	y	distance perpendicular to the wall
c	specific heat	$\bar{\alpha}_e$	average temperature coefficient of electrical resistivity
C	empirical coefficient in Eq. (2)	β	nondimensional mean film thickness ($= \bar{\delta} g^{1/3}/\nu_f^{2/3}$)
d	diameter of probe wire	Γ	mass flow rate per unit film width
g	acceleration due to gravity	δ	film thickness
h	convection heat transfer coefficient	μ	dynamic viscosity
I	electrical current	ν	kinematic viscosity
k	thermal conductivity	ρ	density
L	length of symmetrical half of probe wire	ρ_e	electrical resistivity
L_{lead}	length of lead wire	τ_t	thermal time constant [$= \rho cd/(4h)$]
m	empirical constant in Eq. (2)	**Subscripts**	
Pr	Prandtl number of liquid film	a	air, ambient
q	wall heat flux	f	liquid
R	electrical resistance	s	solid; wire material
R_{ext}	electrical resistance of external circuitry	0	reference condition for resistivity and temperature
R_{lead}	electrical resistance of lead wire		
Re	film Reynolds number ($= 4\Gamma/\mu_f$)	**Overbar**	
Re_d	Reynolds number based on mean film velocity and wire diameter	$\bar{}$	average value; time mean
t	time		
T	temperature		
$T_{s,a}$	steady temperature of wire in air		
$T_{s,\ell}$	steady temperature of wire in liquid		

transport variables can then be defined and averaged with respect to wave coordinates, a coordinate system moving at the velocity of the interfacial waves.

Such simultaneous measurements have never been attempted due, largely, to the small thickness (~ 1 mm) and relatively high frequency of the interfacial waves (up to ~ 100 Hz) on a typical falling film. The hardware required for the measurement of thickness alone is often an obstacle to performing measurements of other transport variables within the film. Accurate determination of the heat transfer coefficient across a falling film, for example, requires heating the film in direct contact with a current-carrying metallic wall, precluding the placement of a conventional electrical admittance (conductance or capacitance) thickness probe directly on the wall.

Reviews of several techniques for film thickness measurement have been presented by Hewitt [1]. However, none of the techniques reviewed is appropriate for heat transfer experiments with a pure, nonconducting liquid (e.g., deionized water) that is in direct contact with an electrically heated wall. The parallel-wire conductance probe is another technique reported by Miya et al. [2], Brown et al. [3], Karapantsios et al. [4], and Koskie et al. [5] as a method for accurate measurement of instantaneous film thickness; however, the need to dissolve an electrolyte in the film precludes the implementation of this technique in the heating of a film on a current-carrying wall.

A technique employing the principle of hot-wire anemometry was used in a needle-contact configuration to measure film thickness in studies by Akai et al. [6] and

Barry [7]. This technique yielded only mean film thickness, which was obtained by integration of the product of probability density of probe contact with liquid and the probe distance from the wall.

The present article describes a new probe for obtaining a continuous time record of film thickness in a dielectric liquid film along with a method for in-situ calibration of the probe. The performance of the thickness probe is examined analytically and numerically. It is shown how this probe facilitates simultaneous transient measurements of film thickness and of temperature across a falling film using a single composite probe assembly, providing new insight into the relationship between interfacial waves and temperature variations in the film.

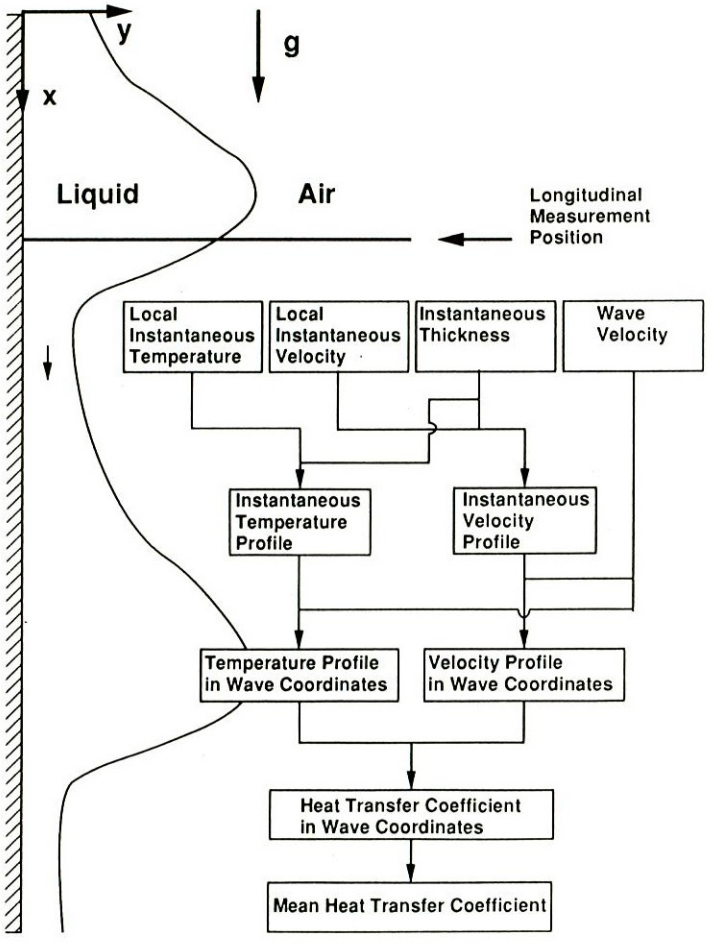

Fig. 1 Determination of the heat transfer coefficient for a falling liquid film using time records of film thickness, liquid temperature, and liquid velocity.

THICKNESS MEASUREMENT TECHNIQUE

Probe Construction

The new thickness probe was designed for obtaining a continuous record of film thickness as a function of time in a dielectric liquid film, a task that could not be accomplished using needle-contact or electrical admittance techniques. Using the new probe, the thickness was determined by measuring the voltage of a small-diameter wire which was stretched across the film as a constant DC current was supplied through the wire.

The thickness-measurement technique was based on two important physical features that resulted in a linear relationship between film thickness and voltage drop across the probe. The first feature is the sensitivity of electrical resistance of a metallic wire to wire temperature. For a wire of length ℓ and cross-sectional area A_c, the resistance R varies with wire temperature T according to the relation

$$R = \frac{\ell}{A_c} \rho_{e,0}[1 + \bar{\alpha}_e (T - T_0)] \tag{1}$$

where $\bar{\alpha}_e$ is the temperature coefficient of resistivity of the wire material and $\rho_{e,0}$ is the volumetric resistivity at a reference temperature T_0. The second feature is the order-of-magnitude difference in the convection heat transfer coefficient in liquid cross-flow over a wire compared to a gas (e.g., air) at the same velocity.

For a small-diameter wire stretched across a liquid–gas interface while supplying a constant DC current, the portion of the wire in the liquid would have a lower electrical resistance per unit length than that in the gas because the relatively large heat transfer coefficient in the liquid maintains the temperature of the wetted portion close to the liquid temperature. On the other hand, the portion of the wire in the gas would be much hotter owing to the poor heat transfer in the gas, resulting in a relatively high electrical resistance per unit length. Thus, fluctuations in the interface would result in a measurable change in the voltage signal because the total electrical resistance is dependent on the lengths of wire segments exposed to the liquid and to the gas.

A schematic of the thickness probe is shown in Fig. 2. The probe was made of 0.0254-mm-diameter (5 to 8 mm long) platinum-10% rhodium wire featuring a high electrical resistivity and a high temperature coefficient of resistivity. The probe was traversed across the film until the probe tip was positioned close to the wall. A protruded section of the fiberglass platform (not shown in Fig. 2) maintained contact with the wall, preventing electrical contact between the probe and the wall. Probe wire selection was made on the basis of maximizing sensitivity to thickness changes while ensuring adequate wire strength. Thermal conductivity, density, and specific heat are also important in selecting the probe wire, since they all influence the thermal response time and Biot number. A small thermal time constant and a small Biot number are both required to minimize time delay in the probe response to film thickness changes. The thickness probe used in the present experiments had a thermal time constant τ_t = 0.09–0.14 ms and Biot number Bi = 0.03 − 0.04 in free-falling water films. The time constant and Biot number were calculated as $\rho_s c_s d/4h$ and $hd/4k_s$, respectively. The heat transfer

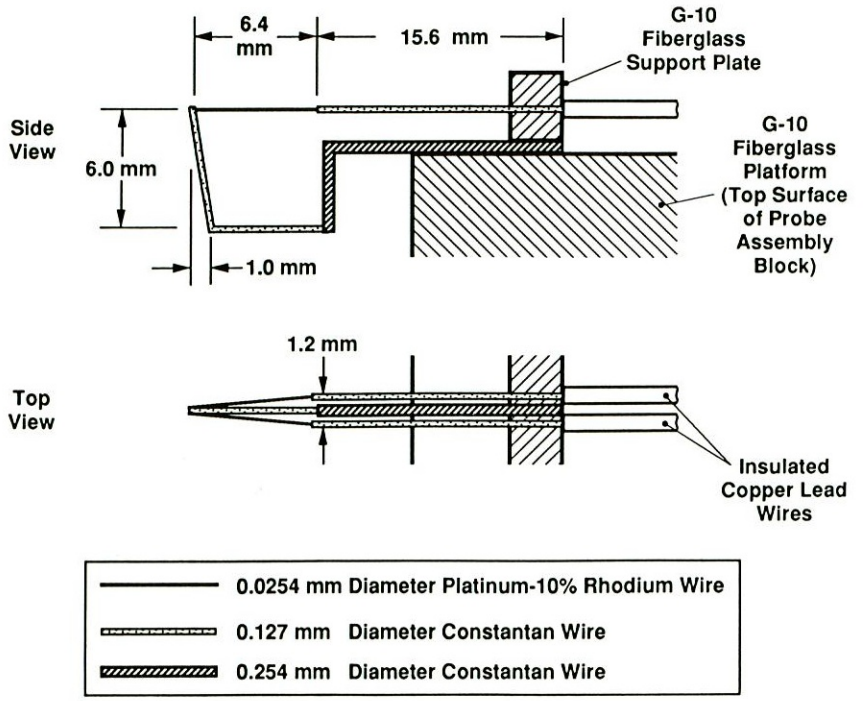

Fig. 2 Construction of the thickness probe.

coefficient, h, was determined from an experimental correlation for cross-flow over a cylinder by Hilpert (see [8]),

$$\frac{hd}{k_s} = C\,\mathrm{Re}_d^m\,\mathrm{Pr}^{1/3} \tag{2}$$

where Re_d is the Reynolds number based on the mean film velocity and wire diameter, and C and m are empirical constants whose values depend on Re_d.

The probe was powered by a KEPCO model ccf 7-2M current regulator by supplying a constant current of approximately 0.2 A through the wire. External noise fluctuations were very small ($\sim$0.03 mV) compared to the voltage signal ($\sim$44 mV/mm) produced by the film thickness changes. Also, the emf (Seebeck voltage) generated by a dissimilar metal junction was too small ($\sim$0.6 mV at 90 °C) to bring about any significant change in the probe signal. Therefore, a clean, high signal-to-noise ratio record of the film thickness was available from direct voltage and current measurements without filtering of the signals. Nevertheless, some noise protection was considered in choosing the lead wire.

One important feature of the thickness measurement is the relatively large temperature difference between segments of the probe located inside and outside of the film. However, this difference may lead to a temperature gradient along the wire near the film interface, producing some uncertainty in the measurement of film thickness. To isolate this effect, one-half of the symmetrical probe was modeled numerically and the steady-

state temperature profile along the probe length was predicted for different film thicknesses in the absence of heating at the wall and interfacial waves. One-dimensional heat conduction was assumed because of the small wire diameter and corresponding low value of wire Biot number. The numerical domain was discretized using the control-volume tridiagonal finite-difference method (see [9]) with a grid size of 0.1 mm. The convection coefficients on the wire segments in air and in liquid (water) were based on correlations for cross-flow over a cylinder, and radiation effects were determined to be negligible. Boundary conditions along the wire included an adiabatic condition at the wall and a prescribed temperature at the end of the lead wire (away from the film interface). These conditions closely simulate film thickness measurements in the absence of heating at the wall. Variations in probe performance in the presence of wall heating will be addressed in a later section.

Figure 3*a* shows the predicted temperature distribution along the wire for three film thicknesses. These results clearly illustrate how the differences in the heat transfer coefficients between the liquid and the air result in a wetted segment at approximately the liquid temperature, and an unwetted segment at a temperature far exceeding that of the air. Another conclusion is that the large temperature gradients associated with the film interface and the solder joint with the thermally insulated lead wire both occur over distances that are insensitive to film thickness. Furthermore, for each of the three cases considered, the temperature gradient at the film interface was confined to the air side, since the high heat transfer coefficient in the liquid was capable of maintaining the wetted segment at a nearly uniform temperature equal to that of the liquid.

The numerical results shown in Fig. 3*a* point to a simple analytical relationship between voltage drop across the probe wire and film thickness in the absence of heating at the wall. Due to symmetry in the probe construction, only one-half of the probe needs to be examined. This relationship can be derived by decomposing the wire length, as shown in Fig. 3*b*, into a segment of length L between the wall and the solder joint with the insulated lead wire, and length L_{lead} of the lead wire. Segment L can also be decomposed into a wetted portion of length equal to the film thickness δ, and an unwetted portion. Temperature gradients are assumed to be present over segments b_ℓ and b_a of the wetted and unwetted portions, respectively, due to axial heat loss near the film interface.

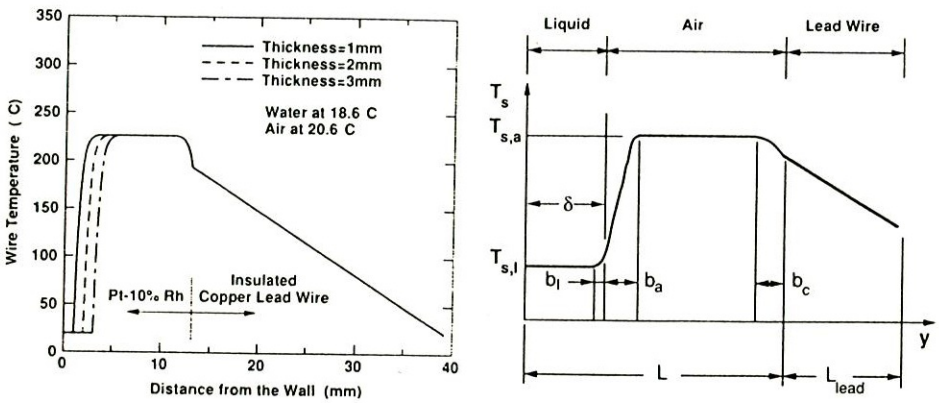

Fig. 3 Variation of wire temperature with distance from the wall for three film thicknesses: (*a*) numerical prediction; (*b*) definition of segment lengths for thickness probe analysis.

Another gradient is also present over a segment b_c of the unwetted portion near the solder joint with the insulated lead wire. A key assumption in the derivation of an expression for film thickness δ as a function of the applied voltage V is that the temperature profiles in segments b_ℓ, b_a, and b_c are invariant with film thickness (except for very small values of δ), as was indeed demonstrated in Fig. 3*a*.

The total electrical resistance of the wire is the sum of the resistances of all its segments,

$$\begin{aligned}\frac{V}{I} &= \int_{\delta-b_\ell} \frac{\rho_{e,0}}{A_c}[1 + \bar{\alpha}_e(T_s - T_0)]\,dz + \int_{b_\ell} \frac{\rho_{e,0}}{A_c}[1 + \bar{\alpha}_e(T_s - T_0)]\,dz \\ &\quad + \int_{b_a} \frac{\rho_{e,0}}{A_c}[1 + \bar{\alpha}_e(T_s - T_0)]\,dz + \int_{L-\delta-b_a-b_c} \frac{\rho_{e,0}}{A_c}[1 + \bar{\alpha}_e(T_s - T_0)]\,dz \\ &\quad + \int_{b_c} \frac{\rho_{e,0}}{A_c}[1 + \bar{\alpha}_e(T_s - T_0)]\,dz + R_{\text{lead}} + R_{\text{ext}} \\ &= \frac{\rho_{e,0}}{A_c}[1 + \bar{\alpha}_e(T_{s,\ell} - T_0)](\delta - b_\ell) + \int_{b_\ell} \frac{\rho_{e,0}}{A_c}[1 + \bar{\alpha}_e(T_s - T_0)]\,dz \\ &\quad + \int_{b_a} \frac{\rho_{e,0}}{A_c}[1 + \bar{\alpha}_e(T_s - T_0)]\,dz + \frac{\rho_{e,0}}{A_c}[1 + \bar{\alpha}_e(T_{s,a} - T_0)](L-\delta-b_a-b_c) \\ &\quad + \int_{b_c} \frac{\rho_{e,0}}{A_c}[1 + \bar{\alpha}_e(T_s - T_0)]\,dz + R_{\text{lead}} + R_{\text{ext}} \end{aligned} \tag{3}$$

where $T_{s,\ell}$ and $T_{s,a}$ are, respectively, the temperatures of the wetted and unwetted segments of the wire maintaining uniform temperature; and R_{lead} and R_{ext} are the resistances of the lead wire and external circuitry, respectively, the sum of which is typically much smaller than V/I. Equation (3) can be rearranged as

$$\begin{aligned}\delta &= \frac{1}{(\rho_{e,0}\,\bar{\alpha}_e/A_c)(T_{s,a} - T_{s,\ell})}\left(-\frac{V}{I} + R_{\text{lead}} + R_{\text{ext}} + \frac{\rho_{e,0}L}{A_c}\right) \\ &\quad + \frac{T_{s,a} - T_0}{T_{s,a} - T_{s,\ell}}L + \int_{b_\ell} \frac{T_s - T_{s,\ell}}{T_{s,a} - T_{s,\ell}}\,dz - \int_{b_a} \frac{T_{s,a} - T_s}{T_{s,a} - T_{s,\ell}}\,dz \\ &\quad - \int_{b_c} \frac{T_{s,a} - T_s}{T_{s,a} - T_{s,\ell}}\,dz \end{aligned} \tag{4}$$

Hence, for a constant current and uniform liquid and air temperatures, the film thickness becomes a linearly decreasing function of applied voltage,

$$\delta = C_1 - C_2 V \tag{5}$$

However, the linearity of Eq. (5) does not hold well for small values of δ, as was mentioned before. Furthermore, the coefficients C_1 and C_2 become calibration constants only for films with equal temperatures.

Equation (5) illustrates how a film thickness calibration relation can be obtained, without prior knowledge of the liquid and air temperatures, from measurements of V and δ corresponding to two different thicknesses. The next section will examine the feasibility as well as limitations of this calibration technique.

Feasibility Tests

Two kinds of feasibility tests were carried out with the thickness probe described in the previous section; one involved measurement of thickness of a stagnant liquid layer and the other a liquid jet. The first test was performed to confirm the linearity in the relationship between voltage and thickness, and also to examine the sensitivity of the measurement. The hardware and instrumentation used in this test are shown in Fig. 4. The platinum-rhodium probe was placed in a small reservoir containing still water. The voltage output and wetted length of the probe wire were recorded at each measurement. One way of controlling the wetted length was to measure the depth of water in the reservoir with a needle contact probe attached to a micrometer. Alternatively, the wetted length was controlled by translating the probe itself with a micrometer. Figure 5 shows the measured voltage varies linearly with film thickness over the range 2 to 7 mm.

In the second feasibility test, the probe was placed just downstream from an adjustable plane wall jet of water, maintaining a constant mean jet velocity as shown in Fig. 6. Figure 7 shows that the relationship between voltage and thickness is fairly linear for this case as well, where the thickness was taken as the width of the jet nozzle. The calibration curve is different from the stagnant water test because of the differences in values of C_1 and C_2 in Eq. (5) between the two tests. The nonlinearity in the wall jet calibration curve, Fig. 7, can be attributed mainly to the deviation of wall jet thickness at the measurement location from the nozzle width. Calibration curves obtained at different

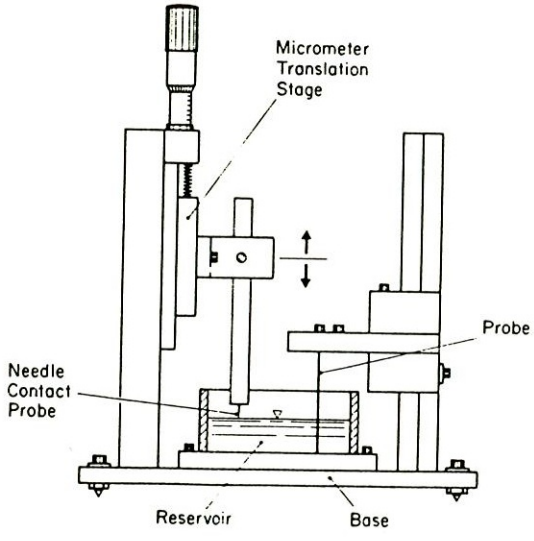

Fig. 4 Stagnant-liquid-layer apparatus used in the probe feasibility tests.

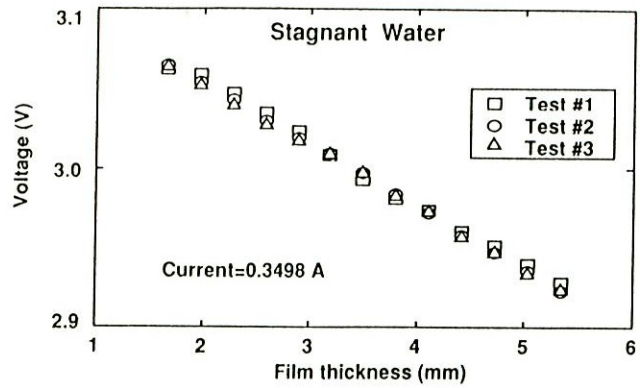

Fig. 5 Variation of the probe voltage with thickness in a stagnant liquid layer.

velocities deviated slightly from the data shown in Fig. 7 and displayed some nonlinearity as well. As indicated earlier, the linearity of Eq. (5) does not hold well for small values of δ due to the boundary layer at the wall reducing the cooling coefficient on the wire in that region. Clearly there exists a small film Reynolds number effect in this calibration, especially for very small film thicknesses.

DYNAMIC CALIBRATION OF THIS THICKNESS PROBE

The previous section described the static calibration of the probe using a steady, predetermined film thickness. In a falling liquid film, the thickness is both transient and difficult to control. Calibrating the thickness probe for this dynamic measurement required the development of a calibration probe that provided a reference signal for the thickness probe. Dynamic calibration was also necessary to account for the temperature changes across the film when heat was supplied form the wall.

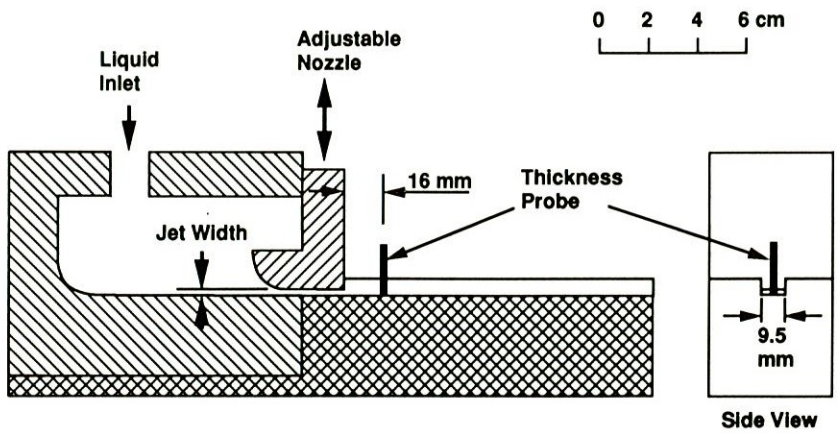

Fig. 6 Wall-jet apparatus used in the probe feasibility tests.

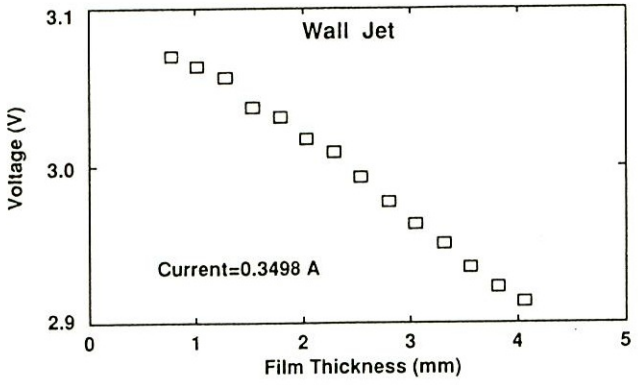

Fig. 7 Variation of the probe voltage with thickness of a wall jet.

Calibration probe operation was based on the same principle as the thickness probe, but it was used only to detect the time of contact between the probe and the film interface. This facilitated calibrating the thickness probe in situ. A schematic of the calibration probe is shown in Fig. 8.

Both the thickness probe and the calibration probe were installed in an experimental apparatus consisting of a 25.4-mm-OD, 1835-mm-long vertical column. Liquid was injected from the inside of a porous tube mounted at the top of the column and allowed to form a film by falling freely on the column outside wall. The column consisted of two parts, an adiabatic section made from G-10 fiberglass, which provided sufficient distance for hydrodynamic development of the film, followed by a 781-mm-long stainless steel section, which conducted a high-DC current, dissipating heat uniformly to the film. Details of the experimental facility can be found elsewhere [10].

During calibration, the thickness probe was translated through the film until it reached a perdetermined distance from the wall, while the calibration probe was trans-

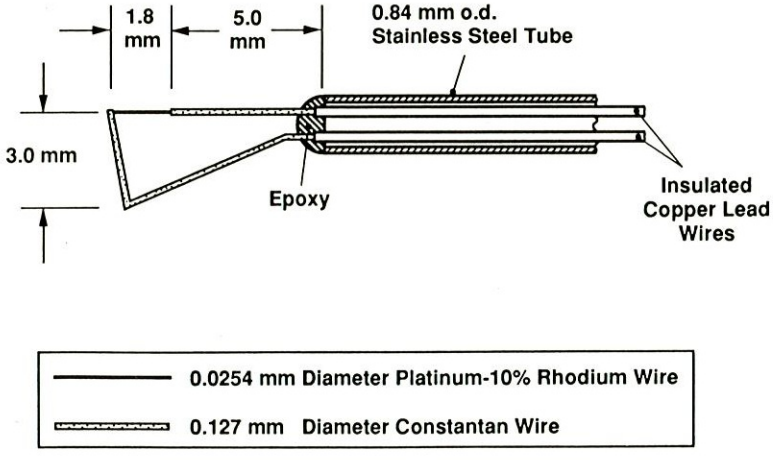

Fig. 8 Construction of the calibration probe.

lated to the calibration distance by a micrometer stage having an accuracy of 0.01 mm. As indicated earlier, a protruding section of the fiberglass platform supporting the thickness probe prevented any electrical contact between the probe and the wall.

The calibration probe was operated with a constant voltage using an HP model 6235A power supply. While the thickness probe produced a continuous signal sensitive to all features of film thickness. the calibration probe experienced only a current surge whenever the liquid made contact with the tip of the probe. Figure 9 shows examples of how calibration data are obtained from comparing signal values from the thickness probe to the corresponding current surges detected by the calibration probe at known distances of the tip of the calibration probe from the wall. In the plot, the error band of the calibration probe signal is not important, because the signal is necessary only to locate the moment of contact. The magnitude of the calibration signal itself is not part of the

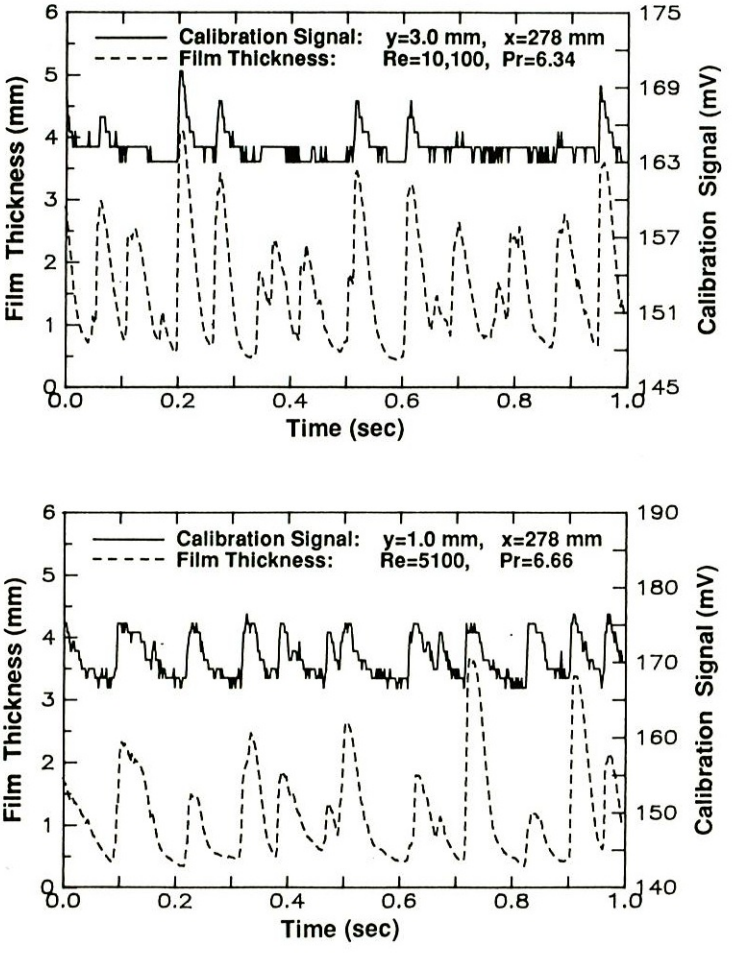

Fig. 9 Signals from the thickness probe and the calibration probe at two distances from the wall.

calibration data. The accuracy of the thickness measurement, including calibration errors, is estimated to be 0.05 mm.

Several calibration data at different calibration probe positions are necessary to correlate the voltage signal of the thickness probe with film thickness. Calibration curves, Fig. 10, were highly linear for thicknesses exceeding 0.75 mm and nonlinear for small thicknesses. The nonlinearity near the wall required careful and extensive calibration of the probe. Since the relationship between thickness probe voltage and thickness is a function of local fluid temperature and velocity, the calibration had to be performed in situ for every set of operating conditions. Although the calibration curves all look quite similar, no attempts should be made to generate a universal calibration curve applicable to all ranges of parameters of a given study. In particular, the calibration curve should not be extended to zero thickness, since the minimum thickness of a liquid film is a function of flow rate.

Measurements of local film thickness were successfully carried out using the thickness probe in heat transfer experiments with deionized water in direct contact with the electrically heated stainless steel wall. Nondimensional mean film thickness data are compared in Fig. 11 with previous data and correlations. The maximum deviations of the mean thickness from correlations by Gimbutis [11] and Takahama and Kato [12] are 16% at Re = 10,400, 9% at Re = 5,200, and 3% at Re = 2,700, respectively. However, the present data are in better agreement with those of Portalski [13] and Karapantsios et al. [4].

SIMULTANEOUS MEASUREMENTS OF FILM THICKNESS AND LIQUID TEMPERATURE

The thickness probe and calibration probe were assembled in an instrumentation block that also carried thermocouples for temperature measurements. The entire block was centered around the stainless steel heated section with the aid of six alignment screws and several translation stages as shown in Fig. 12. Reference data were taken at a location 278 mm from the leading edge of the heated section. Twelve thermocouples made from 0.0508-mm-diameter Chromel and Constantan wires were installed over a 5-mm span on a G-10 plastic knife edge protruding from the instrumentation block to

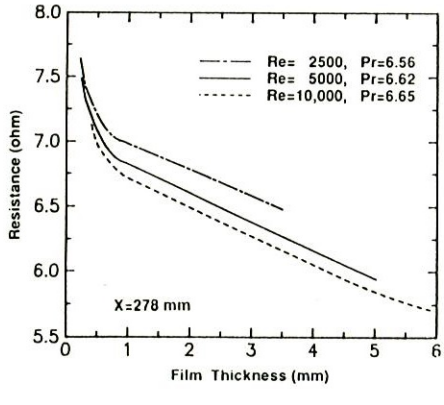

Fig. 10 Thickness probe calibration curves.

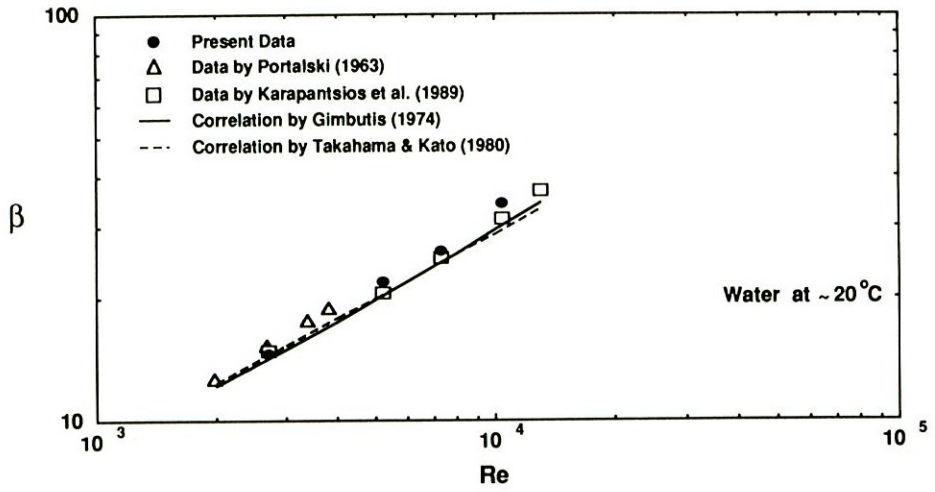

Fig. 11 Comparison of present mean film thickness data with previous correlations and data employing other thickness-measurement techniques.

measure the temperature profile across the film. The thermocouple knife edge and thickness probe were located side by side in the same horizontal plane, as shown in Fig. 12. A high-speed Keithley series 500 data acquisition and control system coupled to a Compaq Deskpro 386 model 40 microcomputer was used to collect film-thickness data along with the liquid temperature data. The data were collected over periods of 1 to 5 s with sampling frequencies ranging from 400 to 500 Hz.

Figure 13 shows three-dimensional plots of temperature distributions across the film as a function of thermocouple distance from the wall, y, and time. The discrete temperature data shown were interpolated using a cubic spline fit. The thickness record can be traced as an outer envelope to the projection of liquid temperature data in the y–t plane. The three plots shown are for a heat flux q = 25,000 W/m^2 and a Prandtl number ranging from 5.64 to 6.82. Increasing Reynolds number from 3,000 to 10,000 significantly increased the convective heat transfer coefficient, as evidenced by the decreasing liquid temperature. Figures 13*a* and 13*b* show a strong correlation between waviness and liquid temperature for the two lower Reynolds numbers, 3,000 and 5,200. The liquid temperature increased within the thin substrate regions of the film separating adjacent large waves and decreased within the large waves. This is due, in part, to the small thermal mass of the substrate causing a relatively large increase in the substrate liquid temperature. At Re = 10,000, Fig. 13*c*, the influence of waviness became negligible as the thicker substrate, stronger intensity of turbulence mixing, and higher frequency of large waves worked together to dampen the temperature fluctuations in the film. A detailed discussion on this topic can be found elsewhere [14].

Figure 13 clearly illustrates the importance of understanding film waviness in the development of accurate models for heat transfer in liquid films. It also demonstrates the usefulness of the newly developed thickness probe and of performing simultaneous measurements of temperature and film thickness toward this goal.

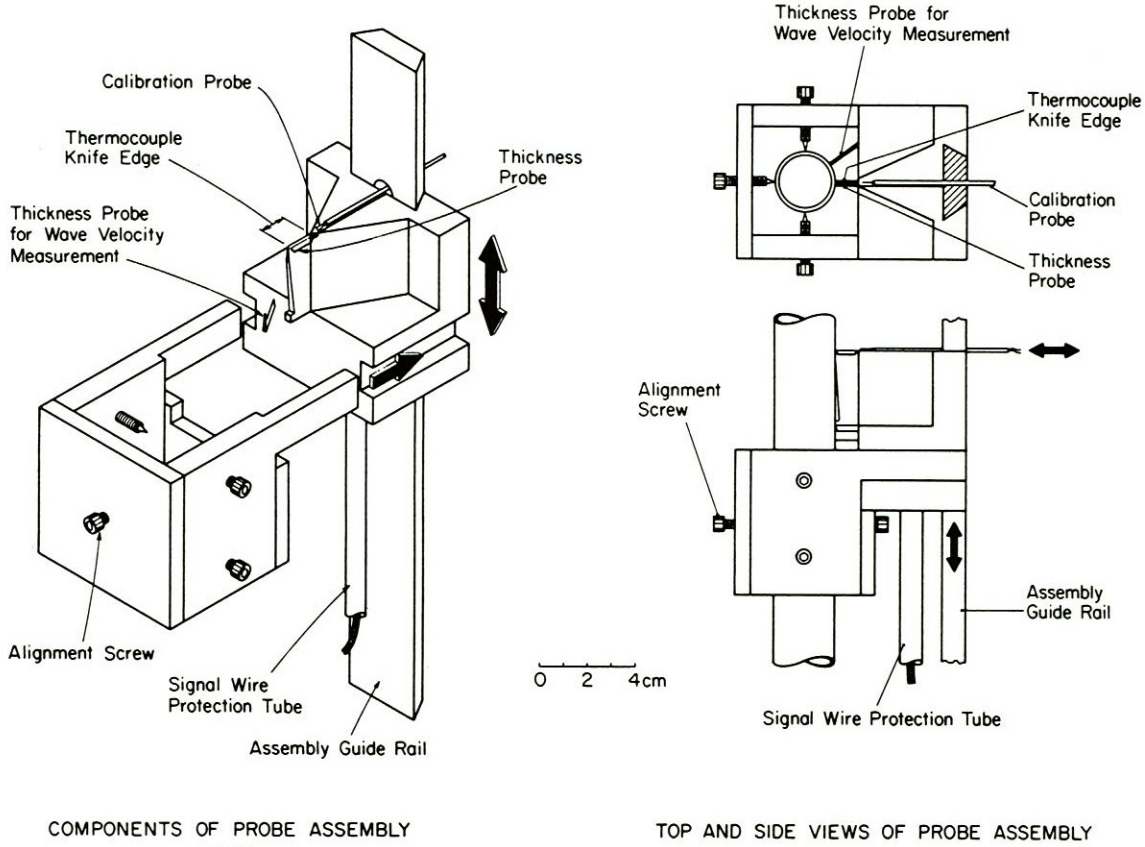

Fig. 12 Probe assembly on the instrumentation block.

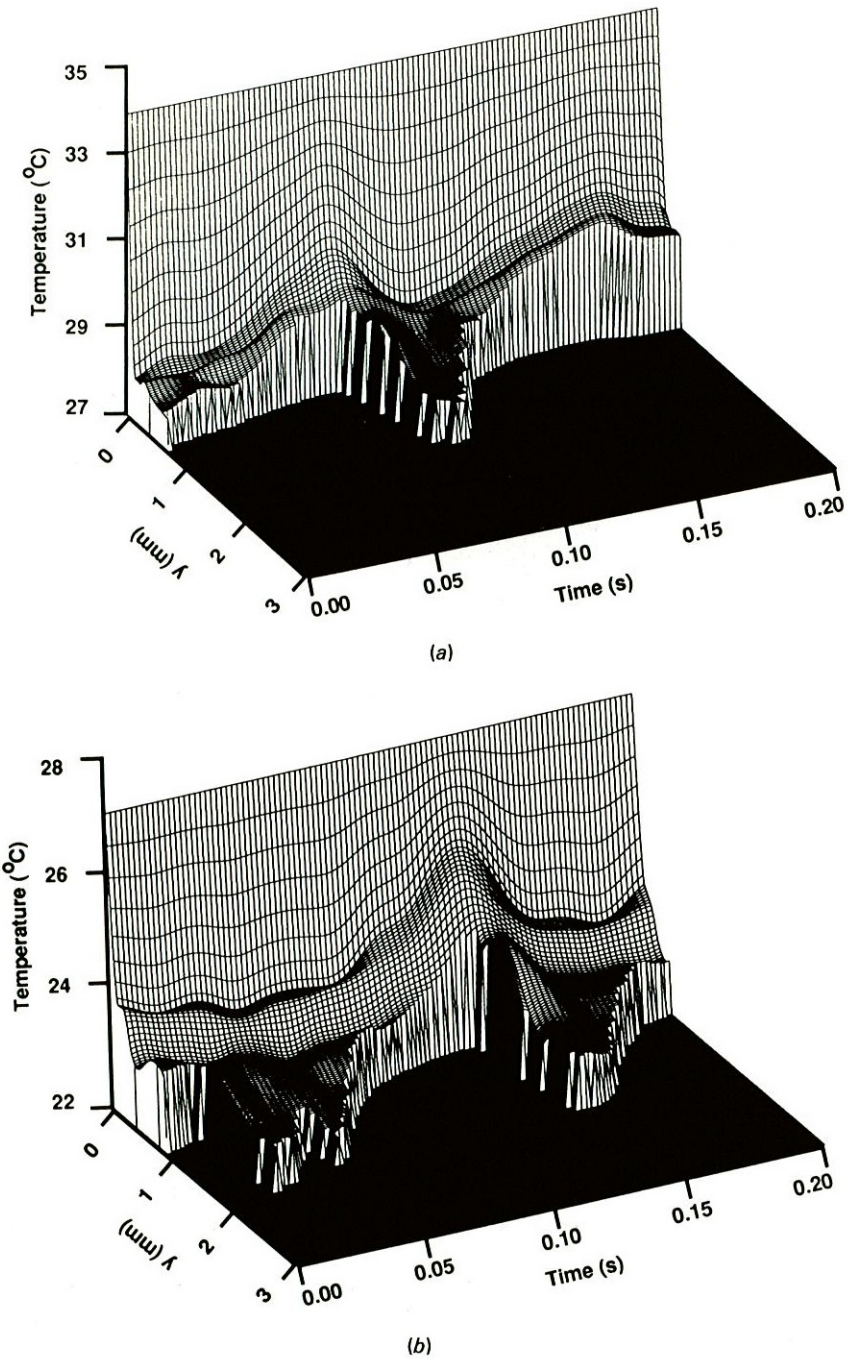

Fig. 13 Three-dimensional plots of liquid temperature with distance from the wall and with time at a heat flux q = 5,000 W/m^2 for: (*a*) Re = 3,000, Pr = 5.64; (*b*) Re = 5,200, Pr = 6.53.

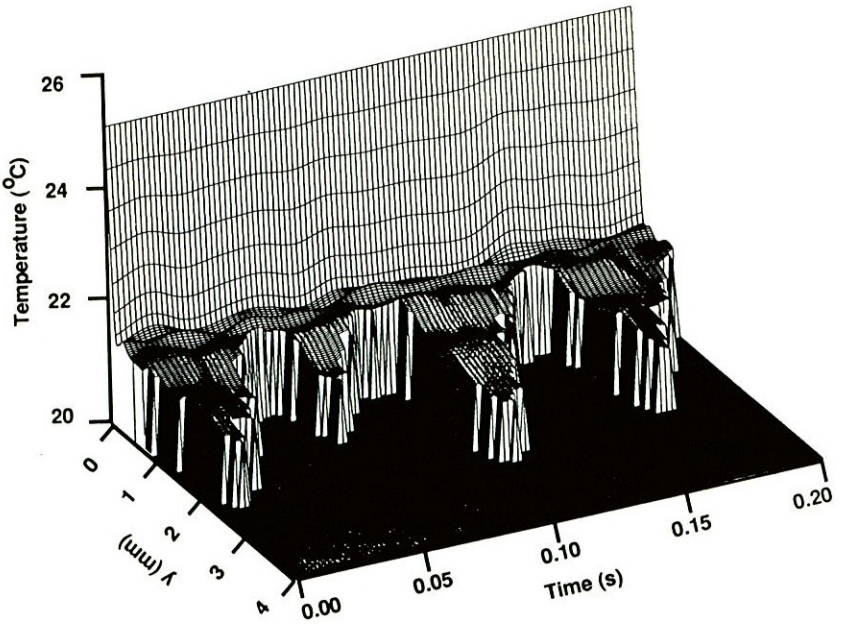

(*c*)

Fig. 13 (*Continued*) Three-dimensional plots of liquid temperature with distance from the wall and with time at a heat flux q = 5,000 W/m^2 for: (*c*) Re = 10,000, Pr = 6.82.

CONCLUSIONS

A new probe was developed for the measurement of film thickness. This article reported the construction and method of calibration of the probe. Also reported was the adaptation of the thickness probe in experiments involving simultaneous measurements of film thickness and temperature profile across the film. The only major drawback of the thickness probe was the need for considerable in-situ calibration, especially for thicknesses smaller than 0.75 mm, for which the relationship between voltage and film thickness becomes nonlinear.

However, the new technique offers many advantages over other thickness measurement techniques. The key advantages are as follows:

1. Unlike all types of electrical admittance thickness probes, the new probe does not require dissolving an electrolyte in the liquid. This makes the new probe adaptable to experiments involving heating of a film that is in direct contact with a current-carrying wall.
2. The new probe produces a continuous time record of film thickness.
3. External noise effects are negligible compared to the large variations in the detected signal. Thus, a clear record is directly available without the need for filtering.
4. The new probe is mounted external to the wall and can be easily relocated for measuring film thickness at different longitudinal locations. External mounting facilitates the adaptation of the probe in heat transfer experiments that preclude

any mechanical alternations to the wall and require the use of other instrumentation for temperature measurement within the film.

REFERENCES

1. G. F. Hewitt, Measurement of Film Thickness, in G. Hetsroni (ed.), *Handbook of Multiphase Systems,* McGraw-Hill, New York, chap. 10, 1982.
2. M. Miya, D. Woodmansee, and T. J. Hanratty, A Model for Roll Waves in Gas-Liquid Flow, *Chem. Eng. Sci.*, vol. 26, pp. 1915–1931, 1971.
3. R. C. Brown, P. Andreussi, and S. Zanelli, The Use of Wire Probes for the Measurement of Liquid Film Thickness in Annular Gas-Liquid Flows, *Can. J. Chem. Eng.*, vol. 56, pp. 754–757, 1978.
4. T. D. Karapantsios, S. V. Paras, and A. J. Karabelas, Statistical Characteristics of Free Falling Films at High Reynolds Numbers, *Int. J. Multiphase Flow,* vol. 15, pp. 1–21, 1989.
5. J. E. Koskie, I. Mudawar, and W. G. Tiederman, Parallel-Wire Probes for Measurement of Thick Liquid Films, *Int. J. Multiphase Flow,* vol. 15, pp. 521–530, 1989.
6. M. Akai, A. Inoue, and S. Aoki, Structure of a Co-current Stratified Two-Phase Flow with Wavy Interface, *Theor. Appl. Mech.*, vol. 25, pp. 445–456, 1977.
7. J. J. Barry, Effects of Interfacial Structure on Film Condensation, Ph.D. thesis, University of Wisconsin—Madison, 1987.
8. F. P. Incropera and D. P. DeWitt, *Fundamentals of Heat and Mass Transfer,* 3rd ed., Wiley, New York, pp. 411–412, 1990.
9. S. V. Patankar, *Numerical Heat Transfer and Fluid Flow,* Hemisphere, Washington, DC, 1980.
10. J. A. Shmerler and I. Mudawar, Local Heat Transfer Coefficient in Wavy Free-Falling Turbulent Liquid Films Undergoing Uniform Sensible Heating, *Int. J. Heat Mass Transfer,* vol. 31, pp. 67–77, 1988.
11. G. Gimbutis, Heat Transfer of a Turbulent Vertically Falling Film, *Proc. 5th Int. Heat Transfer Conf.*, Tokyo, Japan, vol. 2, pp. 85–89, 1974.
12. H. Takahama and S. Kato, Longitudinal Flow Characteristics of Vertically Falling Liquid Films Without Concurrent Gas Flow, *Int. J. Multiphase Flow,* vol. 6, pp. 203–215, 1980.
13. S. Portalski, Studies of Falling Liquid Film Flow: Film Thickness on a Smooth Vertical Plate, *Chem. Eng. Sci.*, vol. 27, pp. 787–804, 1963.
14. T. H. Lyu and I. Mudawar, Statistical Investigation of the Relationship Between Interfacial Waviness and Sensible Heat Transfer to a Falling Liquid Film, *Int. J. Heat Mass Transfer,* in press.